Analyzing Enhancement of CO_2 Reforming of CH_4 in Pd Membrane Reactors

Troy M. Raybold and Marylin C. Huff
Center for Catalytic Science and Technology, Dept. of Chemical Engineering, University of Delaware, Newark, DE 19716

It is demonstrated that H_2 removal through Pd foil membranes can enhance the CO_2 reforming of CH_4. At 550°C and low flows over $Pt/\gamma\text{-}Al_2O_3$ pellets, conversions were twice that of a conventional reactor, while H_2O formation was suppressed, resulting in H_2/CO effluent ratios of 1.0. Larger sweep flows enhanced the reaction somewhat, and the replacement of $Pt/\gamma\text{-}Al_2O_3$ with Pt/ZrO_2 mitigated catalyst deactivation in H_2-poor operating environments. A quantitative correlation was established between reaction enhancement and the overall H_2 removal to production ratio. Based on this correlation, a simple membrane reactor equilibrium model was developed for comparison against experimental data. Subsequently, a unique and useful "on-the-fly" method of gauging membrane limitations, catalyst limitations, and modes of deactivation within a membrane reactor was demonstrated.

Introduction

First investigated by Fischer and Tropsch in 1928, CO_2 reforming of CH_4 (Eq. 1) has been practiced for decades, though primarily in conjunction with steam reforming (Eq. 2) (Bitter et al., 1997)

$$CH_4 + CO_2 \rightleftharpoons 2CO + 2H_2; \quad \Delta H_r^\circ = +247 \text{ kJ/mol} \quad (1)$$

$$CH_4 + H_2O \rightleftharpoons CO + 3H_2; \quad \Delta H_r^\circ = +206 \text{ kJ/mol}. \quad (2)$$

From their early studies, Fischer and Tropsch noted that deactivation by excessive carbon formation on the catalyst surface (i.e., catalyst coking) was a primary obstacle to the success of CO_2 reforming. Both CH_4 decomposition (Eq. 3) and CO disproportionation (Eq. 4) contributed to the observed coking:

$$CH_4 \rightleftharpoons C_s + 2H_2; \quad \Delta H_r^\circ = +75 \text{ kJ/mol} \quad (3)$$

$$2CO \rightleftharpoons C_s + CO_2; \quad \Delta H_r^\circ = -172 \text{ kJ/mol}. \quad (4)$$

Over the past 10–12 years, there has been a surge of academic and industrial interest in further developing stand-alone CO_2, or dry, reforming processes (Ashcroft et al., 1991; Bhat and Sachtler, 1997; Bradford and Vannice, 1998, 1999; Crisafulli et al., 1999; Edwards and Maitra, 1995; Erdohelyi et al., 1993, 1994; Gadalla and Bower, 1988; Gadalla and Sommer, 1989; Gronchi et al., 1997; Halmann and Steinberg, 1999; Hayakawa et al., 1999; Hei, 1998; Kroll et al., 1996, 1997; Krylov et al., 1998; Lu et al., 1998; Mark and Maier, 1996; Matsui et al., 1999; Nakamura et al., 1994; Papp et al., 1996; Rasko and Solymosi, 1997; Raybold, 2000; Rostrup-Nielsen and Bak Hansen, 1993; Slagtern et al., 1997; Solymosi et al., 1991; Stagg et al., 1998; Stagg and Resasco, 1998; Tsipouriari et al., 1994; Wang and Au, 1997; Wang and Lu, 1996, 1998a; Zhang and Verykios, 1994). However, while catalyst deactivation issues are gradually being overcome via these studies, stand-alone dry reforming is still much less mature than other industrial syngas production technologies, such as steam reforming (Adris et al., 1996; Armor, 1999; Hochgesand, 1993; Wittcoff and Reuben, 1996; Woodcock and Gottlieb, 1994), partial oxidation (Armor, 1999; Bharadwaj and Schmidt, 1994; Choudhary et al., 1998; Gomez, 1997; Hickman et al., 1993; Hickman and Schmidt, 1993; Hochgesand, 1993; Hochmuth, 1992; Ito et al., 1999; Lezaun et al., 1998; Marschall and Mleczko, 1999; O'Connor and Ross, 1998; Ruckenstein and Wang, 1999, 2000; Wittcoff and Reuben, 1996; Wolf et al., 1997; Zaera et al., 1999), and autothermal reforming (Armor, 1999; Ellington, 1996). Near-

Correspondence concerning this article should be addressed to M. C. Huff at this current address: Dept. of Chemical Engineering, Drexel University, Philadelphia, PA 19104.
Current address of T. M. Raybold: Praxair, Inc., 175 E. Park Drive, Tonawanda, NY 14151.

term implementations of stand-alone dry reforming are likely to be small scale or newly emerging technologies. For example, three potential "debut niches" for dry reforming include (1) valorization of alternate methane sources such as CO_2-rich natural gas reserves, landfill gas, and biogas (Cook et al., 2000; Harris, 2000; He et al., 1997); (2) production of equimolar syngas for downstream synthesis of acetic acid, formaldehyde, methyl formate, or dimethyl ether (Aparicio, 1997; Bitter et al., 1997; Chen et al., 1997; Edwards and Maitra, 1995; Hochgesand, 1993; Krylov et al., 1998; Lercher et al., 1996; Rostrup Nielsen, 1984; and (3) chemical storage and transportation of energy from renewable sources (Edwards and Maitra, 1995; Hahne, 1993; Levy et al., 1993; Muir et al., 1994; Richardson and Paripatyadar, 1990; Weissermel and Arpe, 1997).

In this article, we discuss the enhancement of the dry reforming reaction through the application of a Pd membrane reactor. Thin foils and films of Pd allow for the exclusive removal of H_2 from a gaseous mixture. By selectively removing H_2 produced by an equilibrium-limited reaction (that is, Eq. 1), equilibrium can be driven toward greater product generation and higher conversions. At a given conversion, membrane reactors can be operated at lower temperatures than corresponding conventional reactors. Besides decreasing energy requirements, lower operating temperatures also reduce the rates of carbon deposition, extending catalyst life. Another advantage of H_2 removal through Pd membranes is the inhibition of the reverse water gas shift reaction (RWGS, Eq. 5):

$$CO_2 + H_2 \rightleftharpoons CO + H_2O; \quad \Delta H_r^\circ = +41 \text{ kJ/mol}. \qquad (5)$$

RWGS is undesirable, as it decreases both H_2 selectivity and the effluent H_2/CO ratio. H_2 removal can suppress this reaction, driving the equilibrium to the left, thereby inhibiting H_2O formation and maintaining equimolar syngas production (that is, H_2/CO ratios ~ 1.0). Other research groups have applied these benefits of selective H_2 removal to the improvement of dry reforming (Galuszka et al., 1998; Ioannides and Verykios, 1996; Kikuchi and Chen, 1997; Ponelis and van Zyl, 1997; Prabhu and Oyama, 1999; Tindall and Grimsehl, 1998).

Experimental Studies

Reaction was conducted within the circular cross-flow membrane reactor depicted in Figure 1. Membrane foils divided the reactor into separate reaction and sweep zones, each 23 cm^3. H_2 permeation could be terminated by replacing the bottom gasket with a solid copper disk. The reactor was heated using electrical-resistance heating tapes and wrapped in insulation to minimize heat losses. Reactor operating temperatures ranged from 550°C to 650°C, with 5–10°C maximum spatial variations.

Reaction-side flow rates ranged from 25 std. $cm^3 \cdot min^{-1}$ to 250 std. $cm^3 \cdot min^{-1}$ (SCCM) at 111.7 kPa. While the N_2 sweep-side flow rate was typically 1000 SCCM at 104.8 kPa, sweep flows from 100 to 5,000 SCCM[3] were considered. Negligible pressure drops were observed on both sides. CO_2/CH_4 feed ratios were maintained at either 1 or 2 with no diluent. All reaction products, except for H_2O, were analyzed using a

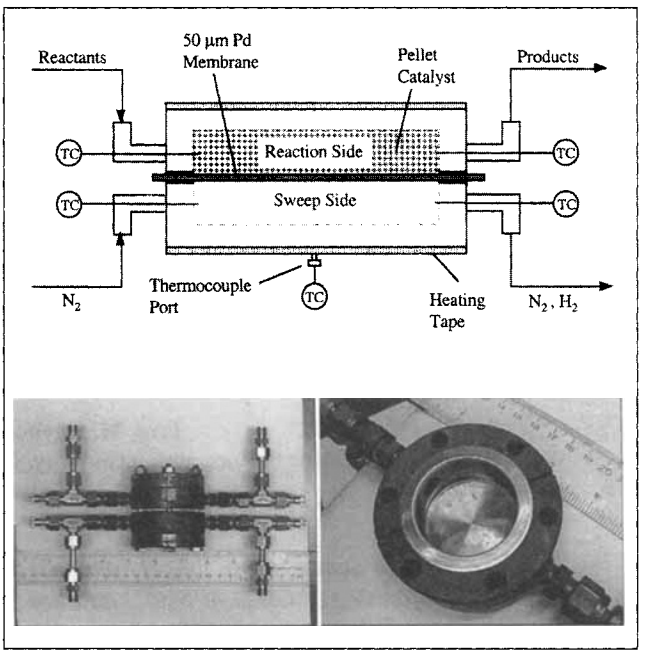

Figure 1. Diagram (top) and photographs (bottom) of the circular cross-flow membrane reactor.

TCD on an HP-6890 GC. Concentrations of H_2O were calculated via an H-atom balance. The C-atom balance served as an internal standard, accounting for mole changes. The remaining O-atom balance closed to within 5% in all cases. Results are summarized by the CH_4 conversion and H_2 selectivity, as defined by Eqs. 6 and 7:

$$X_{CH_4} = \frac{(F_{CH_4})_{in} - (F_{CH_4})_{out}}{(F_{CH_4})_{in}} \times 100 \qquad (6)$$

$$S_{H_2} = \frac{(F_{H_2})_{out,\,sw} + (F_{H_2})_{out,\,r\times n}}{(F_{H_2})_{out,\,sw} + (F_{H_2})_{out,\,r\times n} + (F_{H_2O})_{out,\,r\times n}} \times 100. \qquad (7)$$

The reaction side of the reactor was filled with 0.5 wt. % $Pt/\gamma\text{-}Al_2O_3$ or Pt/ZrO_2 eggshell-coated catalyst pellets. Pure Pd membranes (99.9%, 12 cm^2, 50 μm, Johnson Matthey) were used for all reaction studies. Analysis of membrane permeabilities over a range of temperatures (150–450°C) yielded Arrhenius parameters that closely matched values found in the literature values. Figure 2 presents membrane permeabilities extrapolated from these data to the operating temperatures of interest in this work (500–700°C). Agreement between values from our measurements and those reported in other studies further confirms the well-characterized nature of the fresh Pd membranes (Alefeld and Volkl, 1978; Itoh et al., 1992).

Results and Discussion

Determination of background activity without H_2 removal

Reaction was first conducted in the presence of the Pd membrane, without catalyst. The Pd membrane was placed

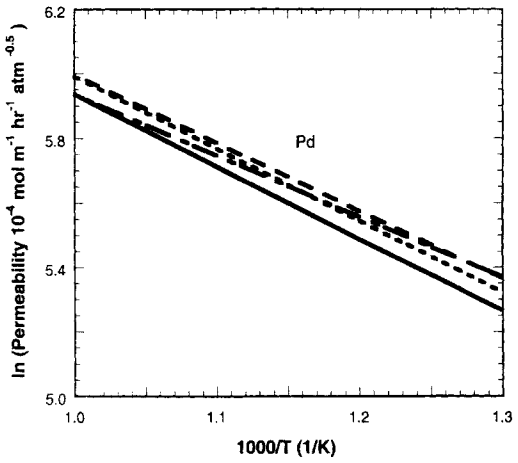

Figure 2. Permeability predictions based on current experimental data (solid) and others (dashed) for Pd from 500 to 700°C (Alefeld and Volkl, 1978; Itoh et al., 1992; Koffler et al., 1969).

on top of a solid copper disk such that no H_2 was removed from the system. We determined the baseline activity attributable to both the Pd foil and the reactor walls at various reaction temperatures, reaction-side flow rates, and inlet CO_2/CH_4 feed ratios. Under none of these conditions did CH_4 conversion rise above 2%. Thus, throughout the rest of this work, we ascribed any reaction to the pellet catalysts.

Confirmation of equilibrium without H_2 removal

If a reaction is not equilibrium-limited, the benefit of a membrane reactor will be significantly reduced or eliminated. Therefore, we sought to determine whether the dry reforming reaction system was indeed equilibrium-limited under the operating conditions of interest. We examined reaction over the Pt/γ-Al_2O_3 pellets in the absence of H_2 removal. Results are presented in Figure 3 for operation between 550 and 650°C, with CO_2/CH_4 ratios of 1.0 and 2.0, and at reaction side flows from 25 to 250 SCCM. Close agreement between the experiments and calculated equilibrium clearly demonstrates that the reaction is equilibrium-limited over the conditions investigated. Larger CO_2/CH_4 feed ratios resulted in greater conversions, but lower H_2 selectivities. The H_2 selectivities generally exhibited greater scatter than the CH_4 conversions, likely due to the additional error involved in calculating the H_2O concentration. Slight excursions above the calculated equilibrium conversions at low reaction side flows are also attributable to experimental error. At higher reaction side flows, minor deviations below equilibrium suggest the onset of kinetic limitations.

Over the course of these experiments, the Pt pellets were exposed to three consecutive intervals (8.5 h each) of operation between 550 and 650°C. CH_4 conversion and H_2 selectivity for a particular operating condition were occasionally monitored over this period, and are presented as Figure 4. This figure indicates that, with no H_2 removal, the Pt/γ-Al_2O_3 catalyst displays stable operation for over 25 h under the given operating conditions.

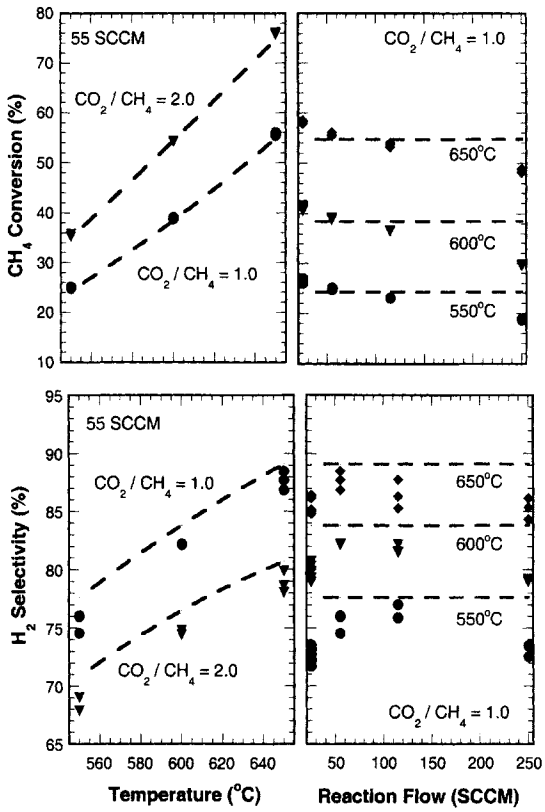

Figure 3. CH_4 conversion (top) and H_2 selectivity (bottom) over a range of operating temperatures (left) and reaction flow rates (right).

Dashed lines represent calculated equilibrium (Pt/γ-Al_2O_3 catalyst, no H_2 removal).

Effect of reaction-side flow with H_2 removal

Since dry reforming is equilibrium-limited under these operating conditions, H_2 removal through the Pd membrane should induce reaction enhancements. Figures 5 and 6 show CH_4 conversion and H_2 selectivity, respectively, over a range of reaction-side flow rates at 550, 600 and 650°C. H_2 removal results in substantial enhancements in both CH_4 conversion and H_2 selectivity, particularly at lower temperatures and flows. For instance, at 25 SCCM and 550°C, CH_4 conversion is twice that of the conventional reactor. Operation at 51% conversion in a conventional reactor would require a reaction temperature of 640°C, indicating a 90°C temperature savings in the membrane reactor. Furthermore, H_2 selectivity is approximately 98%, compared to only 72% in the conventional reactor. That corresponds to a H_2/CO ratio of 0.99 vs. 0.65 in the conventional reactor. As expected, the equilibrium shifts are greatest at the lowest reaction feed flows, where the membrane can remove a greater fraction of the reaction-side H_2. At larger reaction-side flows, the behavior of the membrane reactor asymptotically converges with that of a conventional reactor.

The price for large reaction enhancements, however, is a harsh, H_2-poor reaction environment, which can promote carbon formation and subsequent suppression of catalyst activity and/or membrane permeability. Exposure to such envi-

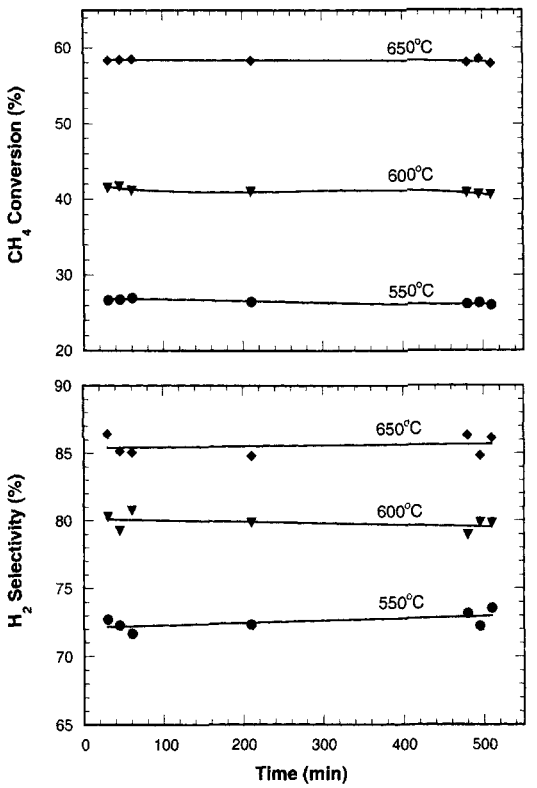

Figure 4. CH_4 conversion (top) and H_2 selectivity (bottom) as a function of time at three operating temperatures (550, 600 and 650°C; ●, ▼, and ♦, respectively) with a CO_2/CH_4 ratio of 1.0 and a reactant flow rate of 25 SCCM (Pt/γ-Al_2O_3 catalyst, no H_2 removal).

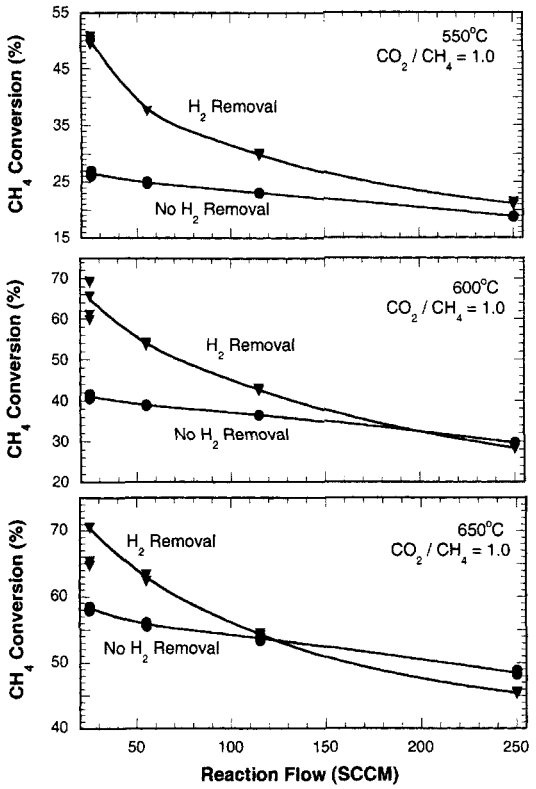

Figure 5. CH_4 conversion over a range of reaction flow rates in the conventional and membrane reactors (●, ▼, respectively) for a CO_2/CH_4 ratio of 1.0, and operating temperatures of 550, 600, and 650°C. (sweep flow = 1,000 SCCM).

ronments for extended periods at these temperatures can even cause the performance of a membrane reactor to eventually fall below that of a conventional reactor. This behavior is observed in the higher temperature plots (600 and 650°C) of Figure 5. Here, increased rates of catalyst deactivation ultimately overwhelm much of the positive membrane effect. The full effect of catalyst and/or membrane deactivation on CH_4 conversion is best illustrated by Figure 7. This figure depicts decreases in CH_4 conversion as a function of time at an operating condition where 80% to 90% of the H_2 produced by reaction is removed. Comparing these results with those of Figure 4 clearly demonstrates that operation in H_2 poor environments presents greater stability problems for both the membrane and catalyst. Possible solutions to these difficulties are discussed briefly in later sections.

Effect of sweep-side flow with H_2 removal

The conversion and selectivity improvements presented earlier were all obtained at a sweep flow rate of 1,000 SCCM. Larger sweep flow rates can increase fluxes by reducing sweep-side H_2 partial pressures. To explore such effects, we examined sweep flow rates from 100 to 5,000 SCCM at both 550 and 650°C (Figure 8). Effects on CH_4 conversion and H_2 selectivity are fairly significant below 1,000 SCCM, but diminish at higher flows. Clearly, beyond a certain point, lowering H_2 partial pressures has little additional value.

Effects of catalyst on deactivation during H_2 removal

We have observed that large rates of H_2 removal result in large equilibrium shifts and reaction enhancements. In fact, these enhancements may permit operation at temperatures almost 100°C lower than required in corresponding conventional reactors. However, we have also observed that large reductions in reaction-side H_2 partial pressures can also exacerbate catalyst coking and deactivation. Thus, to better exploit the effects of H_2 removal, we need a catalyst that is more resistant to coking at low H_2 partial pressures than are the Pt/γ-Al_2O_3 pellets. Conventional catalyst research for dry reforming has indicated that coking can be mitigated by using supports with large oxygen mobilities, such as ZrO_2, CeO_2, or La_2O_3 (Bitter et al., 1997, 1998; Bradford and Vannice, 1997; Hegarty et al., 1998; Kikuchi and Chen, 1997; Lercher et al., 1996; Seshan et al., 1998; Stagg et al., 1998; Stagg and Resasco, 1998). Oxygen mobility allows the support to more effectively dissociate CO_2 and deliver O to the Pt metal for carbon oxidation. We tested eggshell-coated Pt/ZrO_2 pellets under operating conditions that generated a severely H_2-poor reaction environment in which the Pt/γ-Al_2O_3 pellets had deactivated. In Figure 9, CH_4 conversion enhancements (that is, $X_{CH_4,\ membrane}/X_{CH_4,\ conventional}$) are compared over time for both the Pt/γ-Al_2O_3 and the Pt/ZrO_2 pellets. Use of the ZrO_2 support results in a clear improvement in catalyst stability.

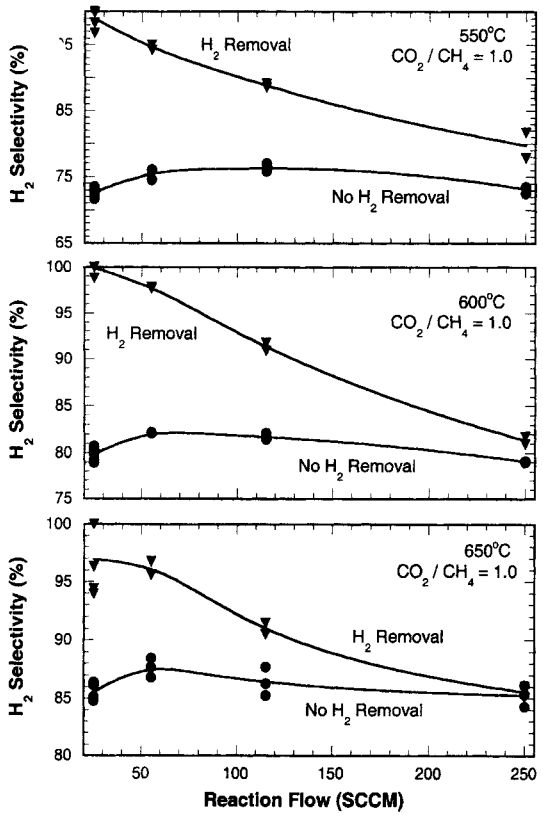

Figure 6. H_2 selectivity over a range of reaction flow rates in the conventional and membrane reactors (●, ▼, respectively) for a CO_2/CH_4 ratio of 1.0, and operating temperatures of 550, 600 and 650°C. (sweep flow = 1,000 SCCM).

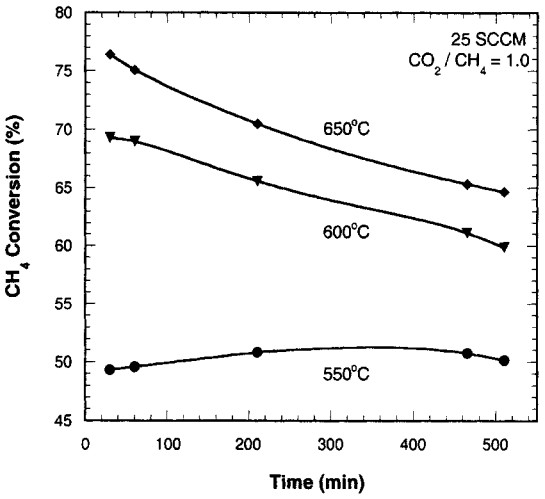

Figure 7. Comparison of CH_4 conversion over time for membrane reactor experiments at three operating temperatures with a reaction flow rate of 25 SCCM and a CO_2/CH_4 feed ratio of 1.0 sweep flow = 1,000 SCCM).

Analysis and Modeling

Reaction enhancements and the balance ratio

Equilibrium shifts (and thus reaction enhancements) are greatest when H_2 production and removal are both sufficiently large and adequately balanced. While this dependence of reaction enhancement on the balance of H_2 production/removal is acknowledged throughout the literature (Deng et al., 1995; Deng and Wu, 1994; Ioannides and Gavalas, 1993; Ioannides and Verykios, 1996; Weyten et al., 1997), it is rarely quantified. In this section, we examine the relationship between these two membrane reactor parameters.

To begin, we define the two quantities of interest (Eqs. 8 and 9)

$$\text{Balance ratio} \equiv \frac{\text{Overall } H_2 \text{ removal}}{\text{Overall } H_2 \text{ production}} \tag{8}$$

$$\text{Reaction enhancement} \equiv \frac{\text{Product yield}_{\text{with } H_2 \text{ removal}}}{\text{Product yield}_{\text{without } H_2 \text{ removal}}}. \tag{9}$$

Of course, conversion and selectivity enhancements may also be defined in a manner analogous to Eq. 9. Experimental measurement of both the balance ratio and reaction enhancements is straightforward. Contained implicitly within the balance ratio are the contributions of reaction flow rates, sweep flow rates, transmembrane pressure gradients, mem-

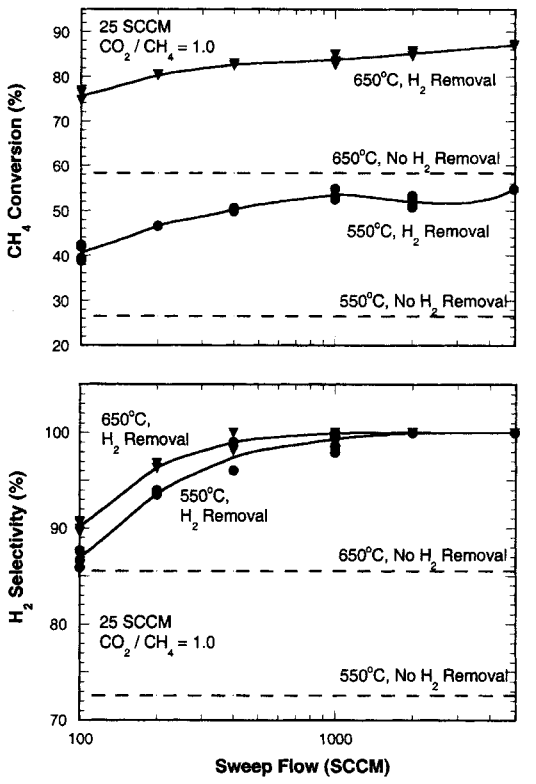

Figure 8. CH_4 conversion (top) and H_2 selectivity (bottom) over a range of sweep flow rates at 550 and 650°C (●, ▼, respectively), CO_2/CH_4 = 1.0, and 25 SCCM reaction flow.

Dashed lines correspond to experimental results with no H_2 removal.

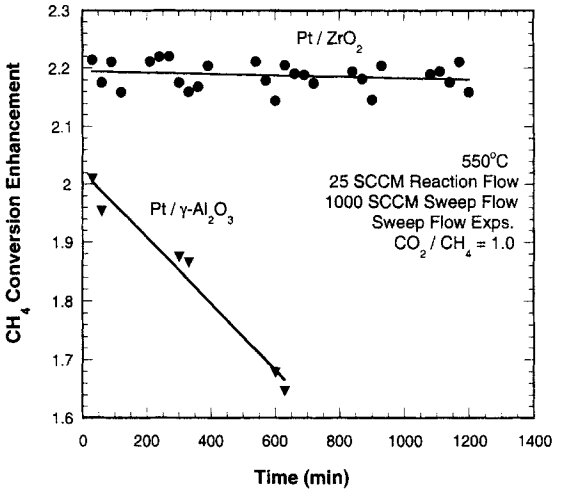

Figure 9. Comparison of CH_4 conversion over time for $Pt/\gamma\text{-}Al_2O_3$ and Pt/ZrO_2 catalysts during sweep flow experiments.

Experimental conditions are noted above.

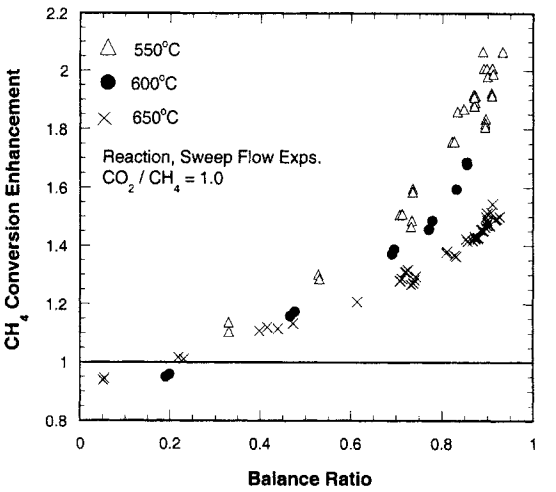

Figure 11. CH_4 conversion enhancements as a function of balance ratios at 550, 600 and 650°C reaction temperatures for a CO_2/CH_4 ratio of 1.0.

Various reaction and sweep flows are represented.

brane permeability, thickness, and surface area, all of which affect the extent of reaction enhancement. As defined, balance ratio values can range from 0 to 1, as one cannot remove more H_2 than produced. Low balance ratios correspond to permeation-limited operation, and generally small

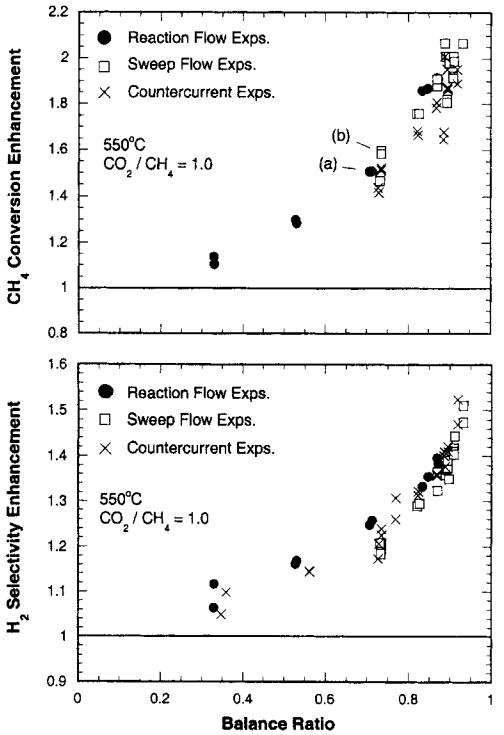

Figure 10. Enhancements of CH_4 conversion (top) and H_2 selectivity (bottom) as affected by balance ratio at 550°C and $CO_2/CH_4 = 1.0$.

Various reaction flows, sweep flows, and flow configurations are represented. Points (a) and (b) are discussed in the text.

reaction enhancements. As the ratio approaches unity, the process comes into balance, and yield enhancements are maximized. Balance ratios of exactly one may indicate a process limited by the rate of H_2 production, where the membrane is not being fully utilized. Overall, the balance ratio can be interpreted as a measure of H_2 removal efficiency.

Figure 10 presents enhancements in CH_4 conversion and H_2 selectivity as functions of a fairly broad range of balance ratios. These data represent experiments at 550°C with equimolar CO_2/CH_4 feeds, but with various sweep flows, reaction flows, and flow configurations. As expected, enhancements in both CH_4 conversion and H_2 selectivity increase as the balance ratio approaches unity. Furthermore, these plots demonstrate that experiments producing similar balance ratios will attain similar conversions, regardless of the specific operating conditions. For example, consider data points (a) and (b) of the top graph in Figure 10, corresponding to ~ 50% conversion enhancements. Point (a) was obtained at a reaction flow of 55 SCCM, with a sweep flow of 1,000 SCCM, while point (b) was obtained at a reaction flow of 25 SCCM, with a sweep flow of 100 SCCM. Similar conversion enhancements are attained because these conditions result in similar balance ratios.

Higher operating temperatures shift the curves to lower reaction enhancements, as indicated in Figure 11. However, this is simply an artifact of the approach to complete conversion. By definition, conversion enhancements become smaller as the conventional equilibrium conversions increase. For instance, equilibrium at 550, 600 and 650°C is 25, 39, and 55%. Thus, the respective maximum attainable enhancements (corresponding to 100% conversion) are 4.0, 2.6, and 1.8. There is also an analogous effect associated with inlet feed ratios (CO_2/CH_4). Figure 12 presents this slight, but consistent downward shift in reaction enhancements. Note that at low balance ratios, enhancements occasionally drop below 1.0. While this is partly attributable to the additional experimental error generated by dividing membrane and conventional reactor conversion data, enhancement factors below unity are

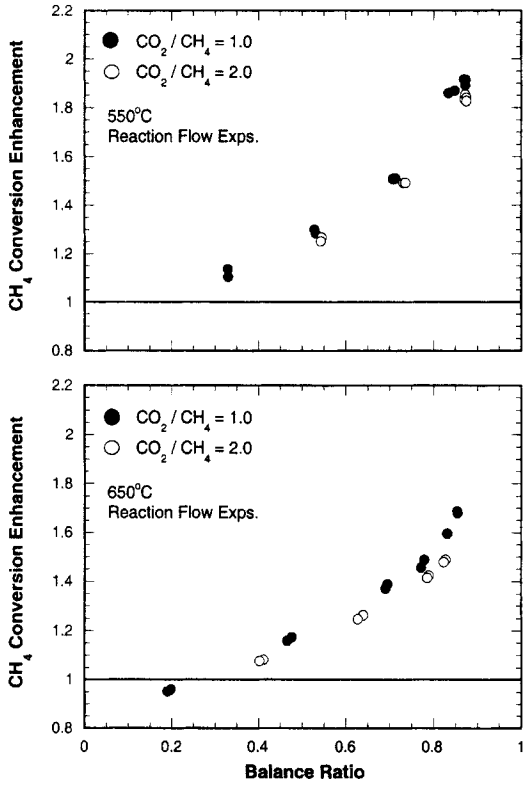

Figure 12. CH_4 conversion enhancement as a function of balance ratio for 550°C (top) and 650°C (bottom) at CO_2/CH_4 feed ratios of 1.0 and 2.0. Various reaction flows are presented at a sweep flow of 1000 SCCM.

possible. Such factors occur if, as discussed earlier, the act of removing H_2 results in an increased deactivation rate that overwhelms the positive membrane effect.

Balance ratios and membrane reactor equilibrium

Most investigations of H_2 removal effects on reaction systems use equilibrium in a conventional reactor as a benchmark. However, it is also useful to quantify the upper limit for such processes: membrane reactor equilibrium. By considering the approach to this upper limit, information can be obtained regarding the effectiveness and appropriateness of the catalyst for membrane reactor operation (Raich and Foley, 1995). Furthermore, by studying transient movement with respect to the equilibrium curve, the competing effects of membrane and catalyst deactivation can be better understood.

Reaction equilibrium assumes infinitely fast reaction velocities (i.e., a proficient catalyst). In a conventional reactor, equilibrium product distributions can be determined through minimization of Gibbs free energy at a given reactor temperature and pressure. For equilibrium in a membrane reactor, we must additionally consider the amount of H_2 removal through the membrane. One simple scenario involves only the selection of a H_2 removal to production ratio (i.e., a balance ratio). With this method, we are not forced to make any explicit assumptions regarding membrane properties, the mechanism of H_2 transport, or fluid dynamics. We need only specify the balance ratio. More details regarding the membrane equilibrium model are provided in the Appendix.

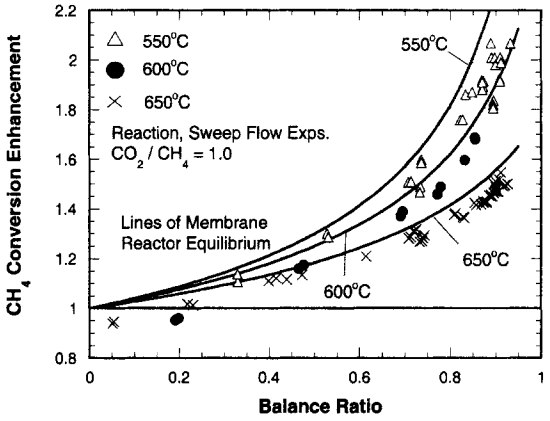

Figure 13. Simulations of CH_4 conversion enhancements at membrane reactor equilibrium with an equimolar CO_2/CH_4 feed for various experiments operated over three reaction temperatures (550, 600, 650°C).

Experimental results are included for comparison.

Simulation results are compared to experimental data in Figures 13 and 14. Note that no fitting of experimental data was used in the generation of these simulations. As expected, the membrane reactor equilibrium model provides an upper bound for the experimental data at each operating temperature and CO_2/CH_4 inlet feed ratio. The model also captures the slight downward shifts caused by increased conversions at both higher temperatures (Figure 13) and greater CO_2/CH_4 feed ratios (Figure 14), which are observed experimentally. Furthermore, the proximity of most of the experimental data to the equilibrium curve implies that the catalyst (Pt/γ-Al_2O_3) is, at least initially, sufficiently active to attain this higher, shifted equilibrium level of reaction. Operation far below the membrane equilibrium curve would imply catalyst deficiencies.

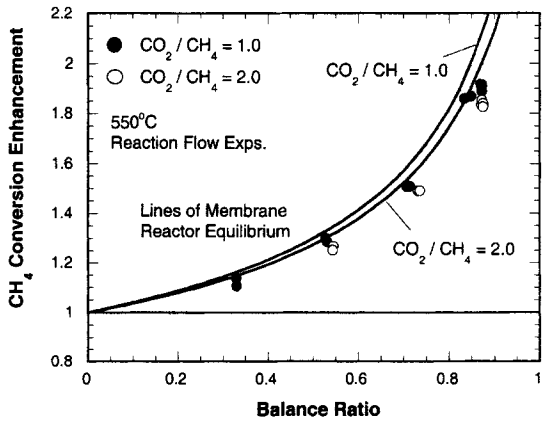

Figure 14. Simulations of CH_4 conversion enhancements under membrane reactor equilibrium at 550°C with CO_2/CH_4 inlet feeds of 1.0 and 2.0.

Experimental results are included for comparison.

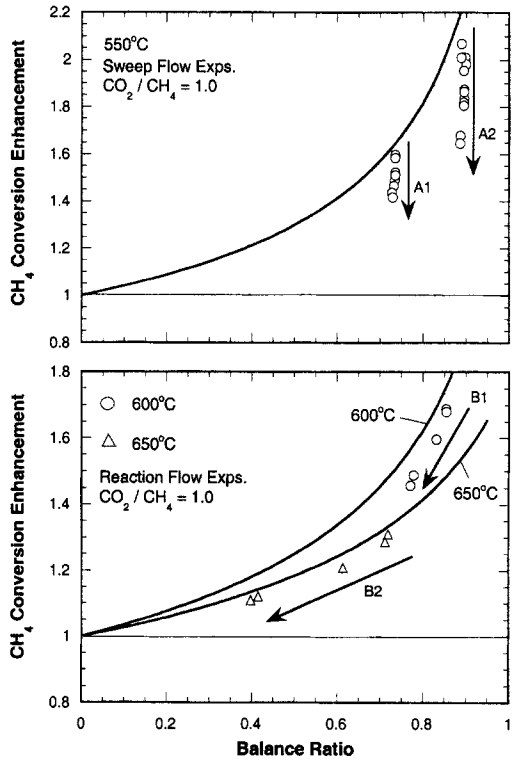

Figure 15. Membrane reactor equilibrium simulations vs. transient data series during sweep (top) and reaction (bottom) flow studies at three different operating temperatures and an equimolar CO_2/CH_4 inlet ratio.

Data series A1, A2, B1, and B2 are discussed in detail in the text. Arrows indicate the progression of time.

Deconvoluting membrane and catalyst deactivation

Reductions in CH_4 conversion (as previously illustrated in Figure 7) may be attributed to catalyst and/or membrane deactivation. In dry reforming, both forms of deactivation are caused by excessive carbon deposition (Goula et al., 1996; Swaan et al., 1994; Wang and Lu, 1998b). Coking of the catalyst reduces activity, while coking of the membrane reduces permeability. Determination of the extent of permeation decay using controlled postreaction H_2 permeation tests may be misleading, as these tests can themselves chemically transform the Pd surface or even remove carbon deposits. This may lead to postreaction permeation values that are not truly indicative of the flux under reaction conditions. However, balance ratio charts allow the visualization of membrane and catalyst deactivation on-the-fly, and furthermore enable the deconvolution of these two forms of deactivation.

By tracking any transient experimental data and comparing these data with the membrane reactor equilibrium curves, the roles of catalyst and membrane deactivation on CH_4 conversion can be further clarified. For instance, in Figure 15, the data series labeled as A1 and A2 correspond to sweep flow rates of 100 and 1000 SCCM, respectively. These two data series were collected during an 8-h examination of a range of sweep flow rates at a temperature of 550°C, an equimolar CO_2/CH_4 feed ratio, and a reactant flow rate of 25 SCCM. These data series exhibit reductions in CH_4 conversions at a constant balance ratio, manifested as vertical drops away from the equilibrium curve. Since balance ratios (H_2 removal efficiencies) remain constant, these vertical drops must correspond to catalyst deactivation.

The data series labeled as B1 and B2 correspond to a reactant flow rate of 25 SCCM at 600 and 650°C, respectively. These two data series were collected during two 8-h examinations of a range of reactant flow rates (25 to 250 SCCM) at an equimolar CO_2/CH_4 feed ratio and a sweep flow rate of 1,000 SCCM. The B1 and B2 data series exhibit CH_4 conversion reductions that appear as tangential "slides" along the equilibrium curve, corresponding to decreases in the balance ratio, or H_2 removal efficiency. Note that the catalyst activity remains sufficiently high to bring the reaction to near-equilibrium compositions under all conditions. Indeed, the catalyst is performing its function quite adequately, while membrane performance degrades.

It seems that a H_2-deficient operating environment is the primary driver for carbon formation and subsequent deactivation. The likely mode of deactivation (i.e., membrane or catalyst) also seems to be somewhat dependent on the balance ratio. When a membrane reactor is operated at low balance ratios, more H_2 remains in the reaction environment, while less is transported through the membrane. This reduction of H_2 transport through the Pd lattice may allow for greater formation of carbon or carbides, which leads to loss of membrane permeability. Conversely, when a membrane reactor is operated at large balance ratios, more H_2 is transported through the membrane, while less remains in the reaction environment. This forces the catalyst to endure long exposures to low H_2 partial pressures. For instance, in the examples considered in Figure 15, the sweep flow experiments that gave rise to data series A1 and A2 had a significantly larger time-weighted average balance ratio value than the reaction flow experiments that gave rise to the B1 and B2 data series.

Of course, in many instances simultaneous membrane and catalyst deactivation will also occur. On a balance ratio plot, such behavior would appear as a movement intermediate between the tangential slide and vertical drop. Of the four data series examined in Figure 15, B1 seems to best exhibit such behavior, as both the balance ratio and the proximity to equilibrium decrease over time.

Conclusions

H_2 removal through Pd membranes can indeed enhance both CH_4 conversion and H_2 selectivity for dry reforming compared to reaction in a conventional reactor, especially at low flow rates or long residence times. At 550°C, conversion and selectivity were enhanced from 26% and 73% to 58% and 99%, respectively. At 650°C, conversion and selectivity were enhanced from 58% and 86% to 88% and 100%, respectively. Such conversion enhancements alternatively translate into almost 100°C reductions in operating temperatures. Furthermore, the RWGS reaction was suppressed, resulting in effluent streams with H_2/CO ratios of 1.0.

Optimal operating conditions involved an equimolar CO_2/CH_4 feed flow of 25 SCCM, with an inert sweep of roughly 1,000 SCCM. Larger reaction flows reduced attain-

able enhancements, while greater sweep flows produced diminishing returns. Pt/ZrO_2 was determined to be slightly more active and much more stable than $Pt/\gamma\text{-}Al_2O_3$ for dry reforming, especially under the H_2-poor reaction environments created by an efficient membrane reactor. However, only relatively short reaction exposures (< 25 h) were considered, and it is conceivable that any catalyst employed in this process would require periodic regeneration. Membrane deactivation was observed under some operating conditions, but seemed to be suppressed when larger amounts of H_2 passed through the Pd foil. Certainly, further material advances producing highly permselective, permeable, and stable membranes could only benefit this process.

We have shown that balance ratio plots are valuable tools for visualizing the state of membrane reactor operation, especially when combined with membrane reactor equilibrium model predictions. The extent of approach to membrane reactor equilibrium can be directly quantified. Furthermore, these plots provide an "on-the fly" deconvolution of the competing effects of membrane and catalyst deactivation on CH_4 conversion or H_2 selectivity. These plots can serve as a much-needed standardized format for presenting membrane reactor results, as currently few researchers quantitatively characterize how well balanced the H_2 production and removal are in their systems. Furthermore, such plots need not be specific to Pd membranes, and could even be applied to membrane addition processes (such as O_2) where balancing reactant addition and subsequent consumption can significantly affect conversions, selectivities, and thermal management.

Literature Cited

Adris, A., B. Pruden, C. Lim, and J. Grace, "On the Reported Attempts to Radically Improve the Performance of the Steam Methane Reforming Reactor," *Can. J. Chem. Eng.*, **74**, 177 (1996).

Alefeld, G., and J. Volkl, *Hydrogen in Metals II: Application Oriented Properties*, Springer-Verlag, New York (1978).

Aparicio, L., "Transient Isotopic Studies and Microkinetic Modeling of Methane Reforming Over Nickel Catalysts," *J. Catal.*, **165**, 262 (1997).

Armor, J., "The Multiple Roles for Catalysis in the Production of H_2," *Appl. Catal. A*, **176**, 159 (1999).

Ashcroft, A., A. Cheetham, M. Green, and P. Vernon, "Partial Oxidation of Methane to Syngas Using Carbon Dioxide," *Nature*, **352**, 225 (1991).

Bharadwaj, S., and L. Schmidt, "Synthesis Gas Formation by Catalytic Oxidation of Methane in Fluidized Bed Reactors," *J. Catal.*, **146**, 11 (1994).

Bhat, R., and W. Sachtler, "Potential of Zeolite Supported Rhodium Catalysts for the CO_2 Reforming of CH_4," *Appl. Catal. A*, **150**, 279 (1997).

Bitter, J. H., K. Seshan, and J. A. Lercher, "The State of Zirconia Supported Platinum Catalysts for CO_2/CH_4 Reforming," *J. Catal.*, **171**, 279 (1997).

Bitter, J. H., K. Seshan, and J. A. Lercher, "Mono and Bifunctional Pathways of CO_2/CH_4 Reforming over Pt and Rh Based Catalysts," *J. Catal.*, **176**, 93 (1998).

Bradford, M., and M. Vannice, "Metal-Support Interactions During the CO_2 Reforming of CH_4 over model TiO_x/Pt Catalysts," *Catal. Lett.*, **48**, 31 (1997).

Bradford, M., and M. Vannice, "CO_2 Reforming of CH_4 over Supported Pt Catalysts," *J. Catal.*, **173**, 157 (1998).

Bradford, M., and M. Vannice, "The Role of Metal-Support Interactions in CO_2 Reforming of CH_4," *Catal. Today*, **50**, 87 (1999).

Chen, Y., K. Tomishige, and K. Fujimoto, "Formation and Characteristic Properties of Carbonaceous Species on Nickel-Magnesia Solid Solution Catalysts During CH_4-CO_2 Reforming Reaction," *Appl. Catal. A*, **161**, L11 (1997).

Choudhary, V., B. Uphade, and A. Mamman, "Simultaneous Steam and CO_2 Reforming of Methane to Syngas over NiO/MgO/SA-5205 in Presence and Absence of Oxygen," *Appl. Catal. A*, **168**, 33 (1998).

Cook, J., M. Neyman, L. Siwajek, and B. Brown, *LFG Use Alternatives*, Acrion Technologies, Inc., Cleveland, OH (2000).

Crisafulli, C., S. Scire, R. Maggiore, S. Minico, and S. Galvagno, "CO_2 Reforming of Methane over Ni-Ru and Ni-Pd Bimetallic Catalysts," *Catal. Lett.*, **59**, 21 (1999).

Deng, J., Z. Cao, and B. Zhou, "Catalytic Dehydrogenation of Ethanol in a Metal-Modified Alumina Membrane Reactor," *Appl. Catal. A*, **132**, 9 (1995).

Deng, J., and J. Wu, "Formaldehyde Production by Catalytic Dehydrogenation of Methanol in Inorganic Membrane Reactors," *Appl. Catal. A*, **109**, 63 (1994).

Edwards, J. H., and A. M. Maitra, "The Chemistry of Methane Reforming with Carbon Dioxide and Its Current and Potential Applications," *Fuel Process. Technol.*, **42**, 269 (1995).

Ellington, R., *Encyclopedia of Chemical Processing and Design*, Dekker, New York (1996).

Erdohelyi, A., J. Cserenyi, E. Papp, and F. Solymosi, "Catalytic Reaction of Methane with Carbon Dioxide over Supported Palladium," *Appl. Catal. A*, **108**, 205 (1994).

Erdohelyi, A., J. Cserenyi, and F. Solymosi, "Activation of CH_4 and Its Reaction with CO_2 over Supported Rh Catalysts," *J. Catal.*, **141**, 287 (1993).

Gadalla, A., and B. Bower, "The Role of Catalyst Support in the Activity of Nickel for Reforming Methane with CO_2," *Chem. Eng. Sci.*, **43**, 3049 (1988).

Gadalla, A. M., and M. E. Sommer, "Carbon Dioxide Reforming of Methane on Nickel Catalysts," *Chem. Eng. Sci.*, **44**, 2825 (1989).

Galuszka, J., R. Pandey, and S. Ahmed, "Methane Conversion to Syngas in a Palladium Membrane Reactor," *Catal. Today*, **46**, 83 (1998).

Gomez, J. P., "Hydrogen Production on Nickel-Monolith Structures by Partial Oxidation of Methane at High Pressure," *Stud. Surf. Sci. Catal.*, **107**, 397 (1997).

Goula, M., A. Lemonidou, and A. Efstathiou, "Characterization of Carbonaceous Species Formed During Reforming of CH_4 with CO_2 over $Ni/CaO\text{-}Al_2O_3$ Catalysts Studied by Various Transient Techniques," *J. Catal.*, **161**, 626 (1996).

Gronchi, P., P. Centola, and R. Del Rosso, "Dry Reforming of CH_4 with Ni and Rh Metal Catalysts Supported on SiO_2 and La_2O_3," *Appl. Catal. A*, **152**, 83 (1997).

Hahne, E., *Ullmann's Encyclopedia of Industrial Chemistry*, VCH, New York (1993).

Halmann, M. M., and M. Steinberg, *Greenhouse Gas Carbon Dioxide Mitigation Science and Technology*, Lewis, New York (1999).

Harris, P., *An Introduction to Biogas*, Report, Univ. of Adelaide, Roseworthy, Australia (2000).

Hayakawa, T., "CO_2 Reforming of CH_4 over Ni Perovskite Catalysts Prepared by Solid Phase Crystallization Method," *Appl. Catal. A*, **183**, 273 (1999).

He, C., D. Herman, R. Minet, and T. Tsotsis, "A Catalytic/Sorption Hybrid Process for Landfill Gas Cleanup," *Ind. Eng. Chem. Res.*, **36**, 4100 (1997).

Hegarty, M., A. O'Connor, and J. Ross, "Syngas Production from Natural Gas Using ZrO_2-Supported Metals," *Catal. Today*, **42**, 225 (1998).

Hei, M., "CO_2-Reforming of Methane on Transition Metal Surfaces," *Surf. Sci.*, **417**, 82 (1998).

Hickman, D. A., E. A. Haupfear, and L. D. Schmidt, "Synthesis Gas Formation by Direct Oxidation of Methane over Rh Monoliths," *Catal. Lett.*, **17**, 223 (1993).

Hickman, D. A., and L. D. Schmidt, "Production of Syngas by Direct Catalytic Oxidation of Methane," *Science*, **259**, 343 (1993).

Hochgesand, G., *Ullmann's Encyclopedia of Industrial Chemistry*, VCH, New York (1993).

Hochmuth, J., "Catalytic Partial Oxidation of Methane over a Monolith Supported Catalyst," *Appl. Catal. B: Environ.*, **1**, 89 (1992).

Ioannides, T., and G. Gavalas, "Catalytic Isobutane Dehydrogenation in a Dense Silica Membrane Reactor," *J. Memb. Sci.*, **77**, 207 (1993).

Ioannides, T., and X. Verykios, "Application of a Dense Silica Membrane Reactor in the Reactions of a Dry Reforming and Partial Oxidation of Methane," *Catal. Lett.*, **36**, 165 (1996).
Ito, M., T. Tagawa, and S. Goto, "Partial Oxidation of Methane on Supported Nickel Catalysts," *J. Chem. Eng.*, Jpn., **32**, 274 (1999).
Itoh, N., W. Xu, and K. Haraya, "Basic Experimental Study on Palladium Membrane Reactors," *J. Memb. Sci.*, **66**, 149 (1992).
Kikuchi, E., and Y. Chen, "Low-Temperature Syngas Formation by CO_2 Reforming of Methane in a Hydrogen-Permselective Membrane Reactor," *Stud. Surf. Sci. Catal.*, **107**, 547 (1997).
Kroll, V., P. Delichure, and C. Mirodatos, "Methane Reforming Reaction with Carbon Dioxide over a Ni/SiO_2 Catalyst: The Nature of the Active Phase," *Kinet. Catal.*, **37**, 698 (1996).
Kroll, V., H. Swaan, S. Lacombe, and C. Mirodatos, "Methane Reforming Reaction with Carbon Dioxide over Ni/SiO_2 Catalyst—II. A Mechanistic Study," *J. Catal.*, **164**, 387 (1997).
Krylov, O., A. Mamedov, and S. Mirzabekova, "Interaction of Carbon Dioxide with Methane on Oxide Catalysts," *Catal. Today*, **42**, 211 (1998).
Lercher, J. A., J. H. Bitter, W. Hally, W. Niessen, and K. Seshan, "Design of Stable Catalysts for Methane-Carbon Dioxide Reforming," *Stud. Surf. Sci. Catal.*, **105**, 463 (1996).
Levy, M., R. Levitan, H. Rosin, and R. Rubin, "Solar Energy Storage Via a Closed Loop Chemical Heat Pipe," *Solar Energy*, **50**, 179 (1993).
Lezaun, J., "Characterization of Ni-Honeycomb Catalysts for High Pressure Methane Partial Oxidation," *Stud. Surf. Sci. Catal.*, **110**, 729 (1998).
Lu, Y., J. Z. Xue, Y. Liu, and S. K. Shen, "Activation of CH_4, CO_2 and Their Reactions over Co Catalyst Studied Using a Pulsed-Flow Micro-Reactor," *React. Kinet. Catal. Lett.*, **64**, 365 (1998).
Mark, M., and W. Maier, "CO_2-Reforming of Methane on Supported Rh and Ir Catalysts," *J. Catal.*, **164**, 122 (1996).
Marschall, K. J., and L. Mleczko, "Short-Contact-Time Reactor for Catalytic Partial Oxidation of Methane," *Ind. Eng. Chem. Res.*, **38**, 1813 (1999).
Matsui, N., "Reaction Mechanisms of Carbon Dioxide Reforming of Methane with Ru-Loaded Lanthanum Oxide Catalyst," *Appl. Catal. A*, **179**, 247 (1999).
Muir, J., R. Hogan, R. Skocypec, and R. Buck, "Solar Reforming of Methane in a Direct Absorption Catalytic Reactor on a Parabolic Dish—Test and Analysis," *Solar Energy*, **52**, 467 (1994).
Nakamura, J., K. Aikawa, K. Sato, and T. Uchijima, "Role of Support in Reforming of CH_4 with CO_2 over Rh Catalysts," *Catal. Lett.*, **25**, 265 (1994).
O'Connor, A. M., and J. R. H. Ross, "The Effect of O_2 Addition on the Carbon Dioxide Reforming of Methane over Pt/ZrO_2 Catalysts," *Catal. Today*, **46**, 203 (1998).
Papp, H., P. Schuler, and Q. Zhuang, "CO_2 Reforming and Partial Oxidation of Methane," *Top. in Catal.*, **3**, 299 (1996).
Ponelis, A., and P. van Zyl, "CO_2 Reforming of Methane in a Membrane Reactor," *Stud. Surf. Sci. Catal.*, **107**, 555 (1997).
Prabhu, A. K., and S. T. Oyama, "Development of a Hydrogen Selective Ceramic Membrane and its Application for the Conversion of Greenhouse Gases," *Chem. Lett.*, **3**, 213 (1999).
Raich, B., and H. Foley, "Supra-Equilibrium Conversion in Palladium Membrane Reactors: Kinetic Sensitivity and Time Dependence," *Appl. Catal. A*, **129**, 167 (1995).
Rasko, J., and F. Solymosi, "Reactions of CH_3 Species with CO_2 on Rh/SiO_2 Catalyst," *Catal. Lett.*, **46**, 153 (1997).
Raybold, T. M., "Novel Applications of Pd-Based Membrane Reactors for Reaction Enhancement," PhD Thesis, Univ. of Delaware, Newark (2000).
Richardson, J., and S. Paripatyadar, "Carbon Dioxide Reforming of Methane with Supported Rhodium," *Appl. Catal.*, **61**, 293 (1990).
Rostrup-Nielsen, J., *Catalysis: Science and Technology*, Springer-Verlag, Berlin (1984).
Rostrup-Nielsen, J., and J. Bak Hansen, "CO_2 Reforming of Methane over Transition Metals," *J. Catal.*, **144**, 38 (1993).
Ruckenstein, E., and H. Y. Wang, "Effect of Support on Partial Oxidation of Methane to Synthesis Gas over Supported Rhodium Catalysts," *J. Catal.*, **187**, 151 (1999).
Ruckenstein, E., and H. Y. Wang, "Partial Oxidation of Methane to Synthesis Gas over MgO-Supported Rh Catalysts: The Effect of Precursor of MgO," *Appl. Catal. A*, **198**, 33 (2000).
Seshan, K., J. H. Bitter, and J. A. Lercher, "Design of Stable Catalysts for Methane Carbon Dioxide Reforming," *Stud. Surf. Sci. Catal.*, **111**, 187 (1998).
Slagtern, A., Y. Schuurman, C. Leclercq, and X. Verykios, "Specific Features Concerning the Mechanism of Methane Reforming by Carbon Dioxide over Ni/La_2O_3 Catalyst," *J. Catal.*, **172**, 118 (1997).
Solymosi, F., G. Kutsan, and A. Erdohelyi, "Catalytic Reaction of CH_4 with CO_2 over Alumina-Supported Pt Metals," *Catal. Lett.*, **11**, 149 (1991).
Stagg, S., E. Romeo, C. Padro, and D. Resasco, "Effect of Promotion with Sn on Supported Pt Catalysts for CO_2 Reforming of CH_4," *J. Catal.*, **178**, 137 (1998).
Stagg, S. M., and D. E. Resasco, "Effect of Promoters on Supported Pt Catalysts for CO_2 Reforming of CH_4," *Stud. Surf. Sci. Catal.*, **110**, 813 (1998).
Swaan, H., V. Kroll, G. Martin, and C. Mirodatos, "Deactivation of Supported Nickel Catalysts During the Reforming of Methane by Carbon Dioxide," *Catal. Today*, **21**, 571 (1994).
Tindall, B., and U. Grimsehl, "The Influence of Temperature and Sweep Gas on Membrane Reactor Performance Using the CO_2 Reforming Reaction," *S. Afr. J. Chem. Eng.*, **10**, 22 (1998).
Tsipouriari, V., A. Efstathiou, Z. Zhang, and X. Verykios, "Reforming of Methane with Carbon Dioxide to Synthesis Gas over Supported Rh Catalysts," *Catal. Today*, **21**, 579 (1994).
Wang, H., and C. Au, "Carbon Dioxide Reforming of Methane to Syngas over SiO_2-Supported Rhodium Catalysts," *Appl. Catal. A*, **155**, 239 (1997).
Wang, S., and G. Lu, "Carbon Dioxide Reforming of Methane to Produce Synthesis Gas over Metal-Supported Catalysts: State of the Art," *Energy Fuels*, **10**, 896 (1996).
Wang, S., and G. Lu, "CO_2 Reforming of Methane on Ni Catalysts: Effects of the Support Phase and Preparation Technique," *Appl. Catal. B: Environ.*, **16**, 269 (1998a).
Wang, S., and G. Lu, "Thermogravimetric Analysis of Carbon Deposition over $Ni/\gamma\text{-}Al_2O_3$ Catalysts in Carbon Dioxide Reforming of Methane," *Energy Fuels*, **12**, 1235 (1998b).
Weissermel, K., and H. J. Arpe, *Industrial Organic Chemistry*, VCH, New York (1997).
Weyten, H., K. Keizer, A. Kinoo, J. Luyten, and R. Leysen, "Dehydrogenation of Propane Using a Packed-Bed Catalytic Membrane Reactor," *AIChE J.*, **43**, 1819 (1997).
Wittcoff, H. A., and B. G. Reuben, *Industrial Organic Chemicals*, Wiley, New York (1996).
Wolf, D., M. Hohenberger, and M. Baerns, "External Mass and Heat Transfer Limitations of the Partial Oxidation of Methane over a Pt/MgO Catalyst-Consequences for Adiabatic Reactor Operation," *Ind. Eng. Chem. Res.*, **36**, 3345 (1997).
Woodcock, K., and M. Gottlieb, *Kirk-Othmer Encyclopedia of Chemical Technology*, 4th ed., Wiley, New York (1994).
Zaera, F., N. R. Gleason, B. Klingenberg, and A. H. Ali, "Partial Oxidation of Hydrocarbons on Nickel: From Surface Science Mechanistic Studies to Catalysis," *J. Mol. Catal. A—Chem.*, **146**, 13 (1999).
Zhang, Z., and X. Verykios, "Carbon Dioxide Reforming of Methane to Synthesis Gas over Supported Ni Catalysts," *Catal. Today*, **21**, 589 (1994).

Appendix: Equilibrium Membrane Reactor Model

The equilibrium membrane reactor model is presented in Figure A1. Initial equilibrium is subsequently followed by alternating steps of H_2 removal and reattainment of equilibrium. Variations of this model were developed by considering different schemes for H_2 removal. In the "balance ratio approach," H_2 removal rates (H_i) are arbitrary, provided that these values are not greater than the H_2 available from the previous equilibrium reactor effluent. H_2 removal is terminated when an equilibrated value of the balance ratio $[(H_{sw}/(H_{sw} + H_{r\times n})]$ reaches some desired, preset limit. Note that the mechanism of H_2 transport need not be assumed nor specified.

Given stream compositions, pressure, temperature, and reaction thermodynamics for the N reactions of interest, equilibrium is determined by solving the set of N nonlinear, cou-

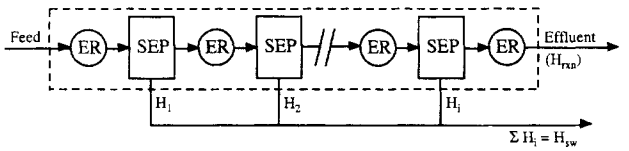

Figure A1. Equilibrium membrane reactor with continuous H_2 removal (ER = equilibrium reactor, and SEP = membrane separator).

pled algebraic equations. The solution is obtained numerically via a modified Powell hybrid algorithm using a finite difference approximation for the Jacobian (that is, IMSL routine NEQNF.F). Example algebraic equilibrium equations for dry reforming (dr) and water gas shift (wgs) are presented as Eqs. A1–A4. In these equations, F_i represents the molar flow of species i, while K_i and ϵ_i are the equilibrium constant and molar extent of reaction for reaction i, and P and T are the absolute pressure (bar) and temperature (K); F_{tot} is the total molar flow, or ΣF_i. Subscripts *MTH*, *CDX*, *CMX*, *HRX*, *WTR*, and *HSW* refer to CH_4, CO_2, CO, reaction side H_2, H_2O, and sweep side H_2, respectively.

$$k_{dr}(bar^2) = \frac{(F_{CMX}+2\epsilon_{dr}-\epsilon_{wgs})^2(F_{HRX}+2\epsilon_{dr}+\epsilon_{wgs})^2(P)^2}{(F_{CDX}-\epsilon_{dr}+\epsilon_{wgs})(F_{MTH}-\epsilon_{dr})(F_{\text{tot}}+2\epsilon_{dr})^2} \tag{A1}$$

$$K_{wgs} = \frac{(F_{CDX}-\epsilon_{dr}+\epsilon_{wgs})(F_{HRX}+2\epsilon_{dr}+\epsilon_{wgs})}{(F_{CMX}+2\epsilon_{dr}-\epsilon_{wgs})(F_{WTR}-\epsilon_{wgs})} \tag{A2}$$

$$K_{dr}(\text{bar}^2) = (0.56)\left\{\exp\left[31{,}224\left(\frac{1}{900}-\frac{1}{T}\right)\right]\right\} \tag{A3}$$

$$K_{wgs} = (2.3)\left\{\exp\left[4{,}307\left(\frac{1}{T}-\frac{1}{900}\right)\right]\right\}. \tag{A4}$$

Manuscript received June 13, 2001, and revision received Oct. 25, 2001.